

Pressure-Induced Superconducting State of Antiferromagnetic CaFe_2As_2

Hanoh Lee¹, Eunsung Park², Tuson Park^{1,2}, F. Ronning¹, E. D. Bauer¹, and J. D. Thompson¹

¹ Los Alamos National Laboratory, Los Alamos, New Mexico 87545, USA

² Department of Physics, Sungkyunkwan University, Suwon 440-746, Korea

(Dated: February 6, 2020)

The antiferromagnet CaFe_2As_2 becomes superconducting under pressure. By measuring electrical resistivity and magnetic susceptibility under pressure, we show that bulk superconductivity is present in a narrow pressure range where collapsed tetragonal and orthorhombic structures coexist. At higher pressures, the collapsed tetragonal structure is stabilized, with the boundary between this structure and the phase of coexisting structures strongly dependent on pressure history. Fluctuations in magnetic degrees of freedom in the phase of coexisting structures appear to be important for superconductivity.

PACS numbers: 74.20.Mn, 74.25.Fy, 74.25.Dw, 74.62.Fj

Discovery of superconductivity in the FeAs-layered compounds $\text{RO}_{1-x}\text{F}_x\text{FeAs}$ (R=La, Nd, Pr, Gd, Sm) has attracted interest because of their high superconducting transition temperatures, which appear to be well outside expectations of a conventional electron-phonon pairing mechanism [1, 2, 3, 4, 5, 6]. Soon after reports of superconductivity in this 'R1111' family of compounds [1], another family of the Fe-As superconductors, AFe_2As_2 (A=Ca, Sr, Ba, Eu), was discovered in which a non-magnetic to antiferromagnetically ordered and tetragonal (T) to low-temperature orthorhombic (O) structural transition take place simultaneously above 100 K [7, 8, 9, 10, 11, 12, 13, 14]. Superconductivity in the A122 family can be induced by electronic doping on the A and Fe sites [15, 16] or by applied pressure [17, 18], and the temperature-pressure phase diagrams for A=Ca, Sr and Ba have been delineated [19]. Because of the relatively low pressures involved, the structural, magnetic and superconducting transition temperatures in CaFe_2As_2 have been studied most extensively as a function of pressure [20, 21, 22]. These experiments have led to conflicting conclusions about the relationship among pressure-induced superconductivity, antiferromagnetic order and structural transitions, open issues that are important to resolve for an interpretation of the physics relevant to superconductivity. By measuring electrical resistivity and magnetic susceptibility under pressure, we find that the temperature-pressure phase diagram of CaFe_2As_2 depends strongly on pressure history and that the superconducting volume fraction peaks in a narrow pressure range. As discussed, these observations suggest that superconductivity emerges as a result of fluctuations associated with the complex state that appears in the pressure interval between approximately 0.3 and 0.8 GPa.

Plate-like single crystals of CaFe_2As_2 , which crystallize in the ThCr_2Si_2 tetragonal structure, were grown from a Sn flux [12]. Electrical resistivity measurements were performed using a conventional four-probe technique with an LR-700 resistance bridge, and ac magnetic suscepti-

bility was measured at 157 Hz using a Stanford Lock-in Amplifier SR830. The resistivity and ac susceptibility of CaFe_2As_2 were measured simultaneously in a clamp-type Be-Cu pressure cell up to 1.52 GPa, where a silicone fluid was used to produce a quasi-hydrostatic pressure environment. Independent studies show [23] that the pressure gradient is less than 0.01 GPa in the structurally glassy state below the fluid's freezing temperature $T_f \approx 122 + aP$, where $a = 87$ K/GPa. The superconducting transition temperature of Pb was measured inductively to determine pressures at low temperature [24]. Several single crystals were studied by electrical resistivity at ambient pressure; crystals with Sn inclusions showed a larger relative resistivity ratio ($\text{RRR} = \rho(300 \text{ K})/\rho(0 \text{ K}) \sim 15$) and those without Sn inclusions had a smaller RRR (~ 5). When both types of samples were subject to pressure, however, characteristic features, such as the structural/antiferromagnetic transition temperature T_S and superconducting transition temperature T_c , were similar to each other. Below, we report data on single crystals CaFe_2As_2 free of Sn inclusions. Though the ambient-pressure RRR (~ 5) was small, it increased to greater than 50 at high pressure, indicating intrinsically high crystallinity with few defects.

Figure 1a displays the electrical resistivity (ρ_{ab}) of CaFe_2As_2 for electrical current flowing in the Fe-As plane. At ambient pressure, there is a step-like, hysteretic increase in the resistivity at 171 K ($=T_S$), where the antiferromagnetic (AFM) and lattice-structural transitions coincide [25]. When cooled through T_S , the high-temperature tetragonal structure switches to an orthorhombic structure and the Fe spin is aligned along the orthorhombic a-axis with an ordered moment $0.8 \mu_B/\text{Fe}$ [20]. Pressure strongly suppresses T_S at an initial rate of -220 K/GPa and the transition width broadens. For pressures higher than 0.35 GPa, where neutron-diffraction measurements found a collapsed tetragonal(cT) structure at 0.63 GPa and 50 K [21], a signature for T_S is hardly visible in the resistivity. In this higher pressure range, muon-spin resonance studies show that

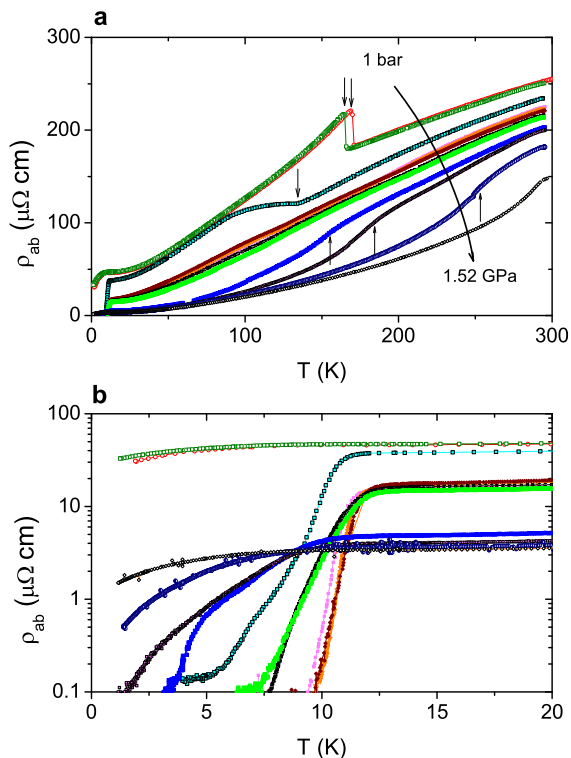


FIG. 1: (color online) Electrical resistivity of CaFe_2As_2 under pressure. **a** In-plane resistivity ρ_{ab} from 1.2 to 300 K for pressures of 1 bar, 0.01, 0.14, 0.41, 0.48, 0.56, 0.7, 0.73, 0.82, 0.98, 1.23, and 1.52 GPa. Arrows denote temperatures for a phase change, as discussed in the text. **b** An expanded view of the low-temperature, in-plane resistivity ρ_{ab} shows the evolution of the superconducting transition temperature T_c . Sharp transitions appear only in a phase of coexisting O and cT structures.

magnetic order persists to at least 0.62 GPa [22]. On the basis of symmetry, magnetic order with the ambient pressure propagation wave-vector must be associated with the O-structure. With further increasing pressure ($P > 0.75$ GPa), a break in the slope of the resistivity (marked by arrows in Fig. 1a) appears, and its temperature increases with increasing pressure, which signals a change to essentially phase-pure cT structure. As shown in Fig. 2a, the transition at T_S^h is strongly hysteretic with temperature, and though not apparent in these figures, the RRR jumps from ~ 15 to over 50 upon entering the new structural phase.

A slight downturn in the resistivity ρ_{ab} of CaFe_2As_2 is observed below 8 K at ambient pressure (Fig. 1b), possibly due to disconnected superconducting filaments. At a pressure of 0.14 GPa, the resistance drops by a factor of 300 at 5.4 K from its value at the SC onset temperature ($=11.5$ K). With further applied pressure, the resistive transition becomes sharp in a narrow pressure range, and the mid-point temperature T_c increases, goes through a maximum near 0.5 GPa and forms a wide pressure dome of T_c 's (circles in Fig. 2b), consistent with an earlier re-

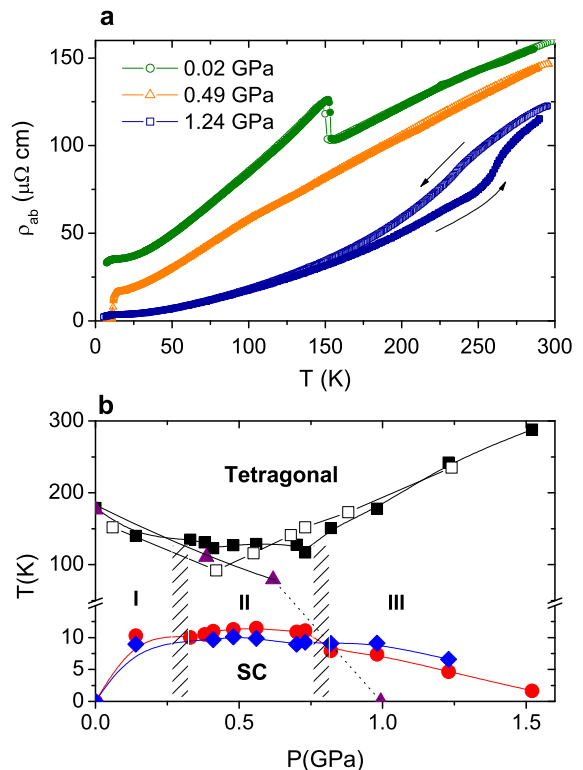


FIG. 2: (color online) **a** Temperature-dependent resistivity in representative pressure ranges, corresponding to those in phases I, II and III in **b**. Note the emergence of strong thermal hysteresis at T_S^h in phase III. **b** Temperature-pressure phase diagram. Solid squares (increasing pressure) denote the structural transition temperature T_S from a tetragonal to an orthorhombic for $P < 0.3$ GPa (phase I), a phase of coexisting O and cT structures for $0.3 < P < 0.8$ GPa (phase II), and the cT structure (phase III) for $P > 0.8$ GPa. Open squares represent structural transitions determined with decreasing pressure. The transition temperatures were defined from a break or maximum in the slope of $d\rho/dT$. Hashed vertical lines separate these structural phases. Circles denote the midpoint of the resistive SC transition and diamonds the onset of superconductivity in ac magnetic susceptibility χ_{ac} . Triangles describe the magnetic transition from a paramagnetic to a SDW phase deduced from μSR measurements [22].

port [18]. Squares in Fig. 2b denote transitions indicated by arrows in Figs. 1a. The existence of superconductivity over a wide pressure range suggests that a specific crystal structure is not a requirement for superconductivity in CaFe_2As_2 , but as will be discussed, this conclusion is not supported by other measurements.

Triangles in Fig. 2b represent the AFM transition (T_N) obtained from μSR measurements [22]. Below 0.3 GPa, both T_N and T_S are suppressed at a similar rate under pressure. For pressures higher than 0.3 GPa, where a collapsed tetragonal structure grows in, the two transitions are decoupled: T_S is almost independent of pressure, but T_N drops rapidly to zero Kelvin between 0.62 and 1.0 GPa. The $T - P$ phase diagram in Fig. 2b shows

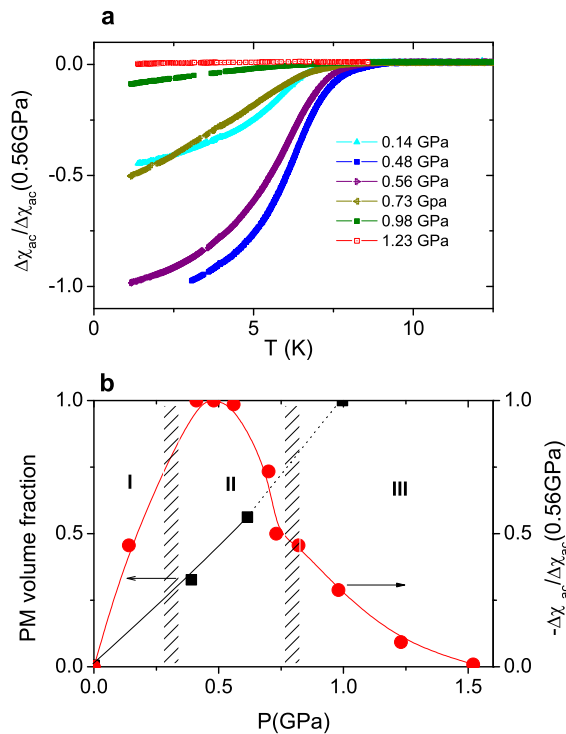


FIG. 3: (color online) **a** Normalized ac magnetic susceptibility $\Delta\chi_{ac}/\Delta\chi_{ac}(=0.56\text{ GPa})$ under pressure, where $\Delta\chi_{ac} = \chi_{ac} - \chi_{ac}(T_c)$. In these units, 1.0 corresponds to at least $0.5(1/4\pi)$ as explained in the text. **b** Diamagnetic response $-\Delta\chi_{ac}(P)/\Delta\chi_{ac}(0.56\text{ GPa})$ (circles) at 1.2 K and volume fraction of a paramagnetic phase estimated by μSR measurements (squares), where the dotted line is an extrapolation [22]. Hashed vertical lines are the same as those shown in Fig. 2b.

the coexistence of magnetism and superconductivity.

The bulk nature of SC was investigated by ac magnetic susceptibility measurements, with results plotted in Fig. 3a. At a pressure close to 1 bar, there is no noticeable change in χ_{ac} (not shown), which is consistent with other bulk measurements. With pressure, a drop in χ_{ac} occurs at the resistive mid-point T_c . The drop, reflecting the volume fraction of superconductivity, initially increases with pressure, goes through a maximum between 0.4 and 0.6 GPa, and becomes negligible at 1.52 GPa (see Fig. 3b). The change in χ_{ac} of CaFe_2As_2 at 0.5 GPa is at least 50 % of perfect diamagnetism based on measurements in the same coil with known superconductors of similar shape and mass, ruling out filamentary superconductivity for CaFe_2As_2 in this pressure range. A similar diamagnetic response is reported in superconducting crystals of $\text{CaFe}_{1.94}\text{Co}_{0.06}\text{As}_2$ [26]. Squares in Fig. 3b represent the pressure evolution of the paramagnetic volume fraction of CaFe_2As_2 estimated from μSR measurements [22]. Neutron-diffraction [27] is consistent with this estimate being an upper limit on the paramagnetic volume fraction. At 0.4 GPa, the superconducting vol-

ume fraction exceeds the paramagnetic volume fraction of the cT phase, indicating that the pressure-induced superconductivity in CaFe_2As_2 is not from a pure, phase-separated paramagnetic phase, but involves much more of the sample volume. A local probe, such as NQR, should verify this conclusion.

Squares in Fig. 4a show the pressure evolution of the residual resistivity (ρ_0) of CaFe_2As_2 , which was obtained from a least-squares fit of the low temperature resistivity to a simple power law, $\rho = \rho_0 + AT^n$. Values of $n(P)$ range between 2 and 3(not shown), but ρ_0 is relatively insensitive to the precise value of n . The residual resistivity displays a sharp change at 0.3 and 0.8 GPa, where O to coexisting O/cT and O/cT to cT structure changes occur, respectively. In the orthorhombic ($P < 0.3\text{ GPa}$) and collapsed tetragonal phase ($P > 0.8\text{ GPa}$), ρ_0 monotonically decreases, but the residual resistivity and T_c are non-monotonic, forming a dome around 0.56 GPa in the coexisting phase $0.3 < P < 0.8\text{ GPa}$ where the diamagnetic response is a maximum. The deviation from a monotonic decrease in ρ_0 signifies an additional scattering mechanism at low temperatures.

The existence of structural and magnetic inhomogeneity in phase II is central to the emergence of bulk superconductivity. We understand this as follows: At the phase I/phase II boundary, domains of cT phase begin to nucleate in the matrix of magnetic O domains, and the relative fraction of these domains reverses as the phase II/phase III boundary is approached. Though scattering at domain walls could account, in part, for the higher ρ_0 in phase II relative to phase III, the density of domain walls would need to be non-monotonic as a function of pressure to account for a maximum in ρ_0 shown in Fig. 4a. This seems unlikely. Alternatively, increased scattering in phase II by dynamical processes provides a more plausible interpretation. The qualitatively lower resistivity over a broad temperature range in the pure cT phase implies a higher density of charge carriers than in the O structure, contrary to naive expectations from band structure calculations that find a reduced density of states in the cT structure [28]. These 'doped' carriers from the cT phase are scattered by fluctuations associated with the O structure. The origin of these fluctuations could be two-fold. In a strong coupling, local-moment picture of the magnetism, magnetic fluctuations are expected as the spin structure of O domains becomes increasingly frustrated due to a pressure-induced increase in As-As and Fe-As hybridization at pressures above 0.3 GPa [29, 30]. On the other hand, in a weak coupling, spin-density-wave model, these changes in hybridization also will modify details of Fermi-surface topology and nesting conditions for the SDW, leading to spin fluctuations from nearly nested parts of the Fermi surface [31]. The correlation between an increase in ρ_0 and T_c as well as the maximum in $-\Delta\chi_{ac}$ in phase II is a consequence of the pressure dependence of the volume

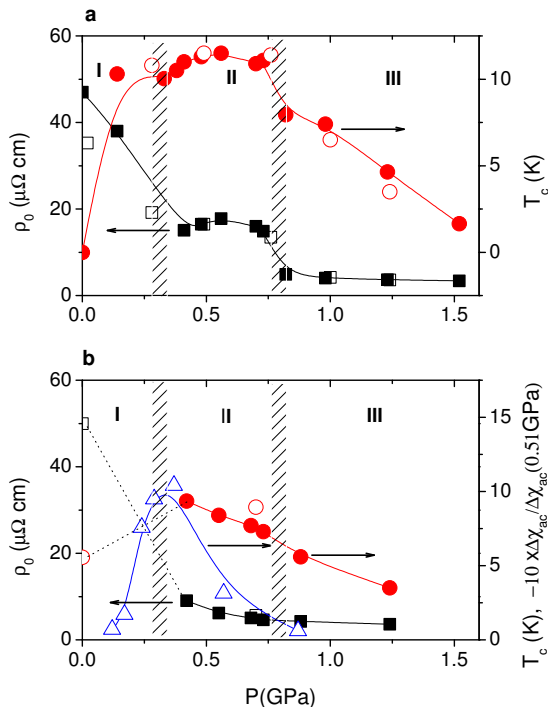


FIG. 4: (color online) **a** Pressure dependence of the residual resistivity ρ_0 (squares) of CaFe_2As_2 plotted on the left ordinate and superconducting transition temperature T_c (circles) plotted on the right ordinate. Solid and open symbols are data obtained with increasing pressure, for the same crystal (#1) reported in previous figures and for a second crystal (#2), respectively. The residual resistivity of #2 was normalized to that of (#1) at 1.2 GPa. Hashed vertical lines are the same as those shown in previous figures. **b** Residual resistivity and resistive mid-point T_c of crystal #1 (solid symbols) and for #2 (open symbols) obtained on decreasing pressure from 1.52 GPa. Open triangles are the normalized diamagnetic response, defined in Fig. 3, for decreasing pressure. Hashed lines from **a** are shown for comparison.

fraction of O and cT, where the O phase is the necessary source of magnetic fluctuations and the cT phase the source of carriers. The coupled spin-'doped' charge dynamics and bulk superconductivity, present only because of structural inhomogeneity, are absent in pure O and cT structures. Whether or not the domain structure is static or dynamic in phase II cannot be established from these experiments, but expected pressure gradients at O/cT domain walls, due to significant structural differences of the phases [21], could favor temporal fluctuations of the domains and Fe moments of the O structure [32]. Without a small (≤ 0.01 GPa) pressure inhomogeneity inevitable with a soft but frozen pressure medium, it is not possible to nucleate the structural inhomogeneity that induces internal strain, which in turn stabilizes the composite structural phases.

The cT phase depends strongly on pressure history, as

shown in Fig. 4b. Decreasing pressure from highest pressures locks in the low residual resistivity of phase III to a pressure much below 0.8 GPa; there is no maximum in ρ_0 for $0.3 \leq P \leq 0.8$ GPa, and the maximum in $-\Delta\chi_{ac}$ appears near 0.3 GPa, all in contrast to results on increasing pressure. Recovery of the initial residual resistivity at ambient pressure suggests that the orthorhombic structure is the stable low temperature structure upon decreasing pressure, as concluded as well in recent structural studies [33]. These conclusions also are consistent with the pressure dependence of T_S determined on decreasing pressure (Fig. 2b). The strong pressure hysteresis of the boundary between phases II and III and large thermal hysteresis at T_S^h will induce structural and electronic inhomogeneities on decreasing pressure and further complicate an interpretation of $T_c(P)$ with decreasing pressure.

In summary, pressure-dependent resistivity and ac susceptibility measurements reveal strong coupling among superconductivity, structure and magnetism in CaFe_2As_2 . The coexisting phase, which exists in a narrow window of increasing pressure, supports bulk superconductivity due to the coupled spin-charge dynamics special to the coexistence.

Note added: After initially submitting this paper, measurements [34] in a more nearly hydrostatic environment showed that there is no phase II and no bulk superconductivity, results fully consistent with our conclusions.

We thank V. A. Sidorov for characterizing the hydrostaticity of our pressure medium. Work at Los Alamos was performed under the auspices of the U.S. Department of Energy/Office of Science and supported by the Los Alamos LDRD program. EP and TP acknowledges a grant from the Korea Science and Engineering Foundation (KOSEF) funded by the Korea government R01-2008-000-10570-0.

-
- [1] Y. Kamihara, T. Watanabe, M. Hirano, and H. Hosono, *J. Am. Chem. Soc.* **130**, 3296 (2008).
 - [2] X. H. Chen *et al.*, *Nature* **453**, 761 (2008).
 - [3] Z.-A. Ren *et al.*, *Europhys. Lett.* **82**, 57002 (2008).
 - [4] Z.-A. Ren *et al.*, *Materials Research Innovations* **12**, 106 (2008).
 - [5] R. H. Liu *et al.*, *Phys. Rev. Lett.* **101**, 087001 (2008).
 - [6] I. I. Mazin, D. J. Singh, M. D. Johannes, and M. H. Du, *Phys. Rev. Lett.* **101**, 057003 (2008).
 - [7] M. Rotter *et al.*, *Phys. Rev. B* **78**, 020503(R) (2008).
 - [8] N. Ni *et al.*, *Phys. Rev. B* **78**, 014507 (2008).
 - [9] J.-Q. Yan *et al.*, *Phys. Rev. B* **78**, 024516 (2008).
 - [10] C. Krellner *et al.*, *Phys. Rev. B* **78**, 100504(R) (2008).
 - [11] G. F. Chen *et al.*, *Chin. Phys. Lett.* **25**, 3403 (2008).
 - [12] F. Ronning, T. Klimczuk, E. D. Bauer, H. Volz, and J. D. Thompson, *J. Phys.: Condens. Matter* **20**, 322201 (2008).
 - [13] G. Wu *et al.*, arXiv:0806.4279 (unpublished).

- [14] N. Ni *et al.*, Phys. Rev. B **78**, 014523 (2008).
- [15] M. Rotter, M. Tagel, and D. Johrendt, Phys. Rev. Lett. **101**, 107006 (2008).
- [16] A. S. Sefat *et al.*, Phys. Rev. Lett. **101**, 117004 (2008).
- [17] T. Park *et al.*, J. Phys.: Condens. Matter **20**, 322204 (2008).
- [18] M. S. Torikachvili, S. L. Bud'ko, N. Ni, and P. C. Canfield, Phys. Rev. Lett. **101**, 057006 (2008).
- [19] P. L. Alireza *et al.*, arXiv:0807.1896 (unpublished).
- [20] A. I. Goldman *et al.*, Phys. Rev. B **78**, 100506(R) (2008).
- [21] A. Kreyssig *et al.*, arXiv:0807.3032 (unpublished).
- [22] T. Goko *et al.*, arXiv:0808.1425 (unpublished).
- [23] V. A. Sidorov, unpublished.
- [24] A. Eiling and J. S. Schilling, J. Phys. F.: Metal Phys. **11**, 623 (1981).
- [25] S.-H. Baek *et al.*, arXiv:0808.0744 (unpublished).
- [26] N. Kumar *et al.*, arXiv:0810.0848v2 (unpublished).
- [27] A. I. Goldman *et al.*, arXiv:0811.2031v1 (unpublished).
- [28] T. Yildirim, arXiv:0807.3936 (unpublished).
- [29] T. Yildirim, Phys. Rev. Lett. **101**, 057010 (2008).
- [30] M. J. Han, arXiv:0811.0034v1 (unpublished).
- [31] For example, V. Stanev, J. Kang and Z. Tesanovic, Phys. Rev. B **78**, 184509 (2008).
- [32] I. I. Mazin and M. D. Johannes, arXiv:0807.3737 (unpublished).
- [33] A. I. Goldman *et al.*, arXiv:0811.2013v2 (unpublished).
- [34] W. Yu *et al.*, arXiv:0811.2554v1 (unpublished).